Provided for non-commercial research and education use.
Not for reproduction, distribution or commercial use.

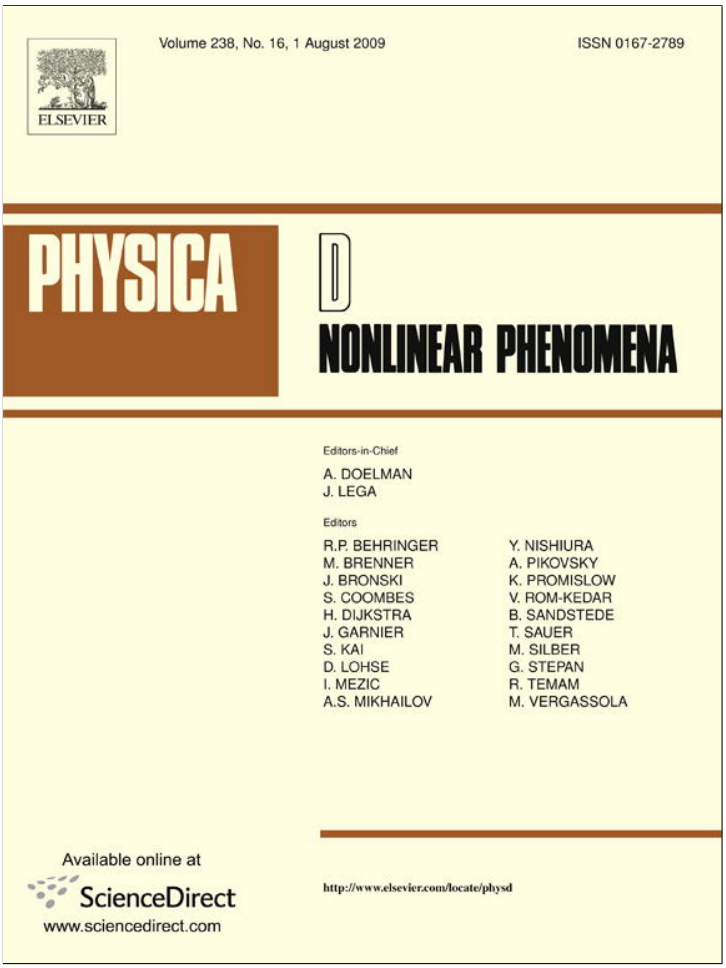

This article appeared in a journal published by Elsevier. The attached copy is furnished to the author for internal non-commercial research and education use, including for instruction at the authors institution and sharing with colleagues.

Other uses, including reproduction and distribution, or selling or licensing copies, or posting to personal, institutional or third party websites are prohibited.

In most cases authors are permitted to post their version of the article (e.g. in Word or Tex form) to their personal website or institutional repository. Authors requiring further information regarding Elsevier's archiving and manuscript policies are encouraged to visit:

http://www.elsevier.com/copyright

Author's personal copy

Physica D 238 (2009) 1561–1568

Contents lists available at ScienceDirect

Physica D

journal homepage: www.elsevier.com/locate/physd

Autoresonant excitation of multiphase waves in the sine-Gordon model

A.G. Shagalov [a], L. Friedland [b,*]

[a] Institute of Metal Physics, Ekaterinburg 620041, Russian Federation

[b] Racah Institute of Physics, Hebrew University of Jerusalem, Jerusalem 91904, Israel

ARTICLE INFO

Article history:
Received 19 August 2008
Received in revised form
8 April 2009
Accepted 17 April 2009
Available online 3 May 2009
Communicated by V. Rom-Kedar

PACS:
89.75.Kd
05.45.Yv
05.45.Xt

Keywords:
Multiphase waves
Sine-Gordon equation
Autoresonance
Inverse scattering transform method

ABSTRACT

Autoresonant excitation and control of multiphase waves of the sine-Gordon equation is discussed. The autoresonance (a persistent nonlinear phase-locking) is achieved by applying chirped frequency wave-like perturbations and passage through resonances with inactive (dormant) degrees of freedom in the system. Successful phase locking requires the amplitude of the driving perturbation to exceed a threshold that scales as 3/4 power of the driving frequency chirp rate. The spectral theory of the inverse scattering transform method is used for diagnostics and analysis of the excited solutions.

© 2009 Elsevier B.V. All rights reserved.

1. Introduction

The sine-Gordon (SG) equation

$$u_{tt} - u_{xx} + \sin u = 0 \tag{1}$$

is one of the most important equations of nonlinear physics and describes many physical applications [1]. It has a variety of solutions, the simplest being a single-phase wave train, $u = u(\Theta)$, $\Theta = \kappa x - \omega t$. Other examples are standing waves of form $u = 4\tan^{-1}[F(x)G(t)]$ [2] in the periodic problem, $u(x + L) = u(x)$, where F and G are expressed in terms of Jacobian elliptic functions. Well known realizations of such standing waves are the breather and plasma oscillations [3]. More complex solutions of the sine-Gordon equation comprise multiphase waves of form

$$u(x, t) = u(\Theta_1, \ldots, \Theta_N), \qquad \Theta_i = \kappa_i x - \omega_i t + \Theta_{0i},$$

where the wave vectors κ_i are multiples of $k_0 = 2\pi/L$. A complete description of such solutions can be obtained via the Inverse Scattering Transform (IST) method [4,5]. Generation of the multiphase waves in physical systems is difficult because it requires the realization of complicated initial conditions. The present study discusses another possibility of formation and control of such solutions, i.e., the autoresonant excitation from zero by applying plane wave-like perturbations passing through resonances in the system. Thus, we focus on the perturbed sin-Gordon equation

$$u_{tt} - u_{xx} + \sin u = \epsilon f(x, t) \tag{2}$$

where $f(x, t) = \cos\left(\kappa_m x - \int \Omega_m(t)\mathrm{d}t\right)$, $\kappa_m = \frac{2\pi}{L}m$, $\epsilon \ll 1$, and the driving frequency $\Omega_m(t)$ is a slow function of time. The ac-driven SG system was studied in the past for constant frequency drives [6]. The idea of passage through and capture into resonance for controlling SG waves was suggested later in applications to single-phase SG waves [7], mode conversion in a system of coupled SG equations [8], and formation of breather and plasma oscillations [9]. Autoresonance is a salient feature of many nonlinear systems to stay in resonance (dynamically phase-lock) with driving perturbations even if the systems' parameters vary in time [10–13]. This continuing phase-locking means excursion in the driven systems parameter space, i.e. control of the phase-locked solution by an external parameter (the driving frequency). Here we extend this approach to excitation of more general, multiphase solutions in the SG problem. Previously autoresonant multiphase waves were studied for the periodic Toda chain, the Korteweg–de-Vries, and Nonlinear Schrodinger equations (see [14] and references therein). Our presentation will be as follows. In Section 2, as a background material, we will describe the spectral

* Corresponding author. Tel.: +972 2 658 5612; fax: +972 2 658 5257.
E-mail address: lazar@vms.huji.ac.il (L. Friedland).

0167-2789/$ – see front matter © 2009 Elsevier B.V. All rights reserved.
doi:10.1016/j.physd.2009.04.013

Author's personal copy

IST problem associated with the unperturbed SG problem. The IST method is much more effective for analyzing multiphase waves than other traditional approaches (e.g. time Fourier spectra at a given point x), especially when the wave parameters are slowly varying in time. Indeed, the number of the components in the IST spectrum of the periodic sine-Gordon problem is twice the number of the frequencies ω_i in the solution (see Section 2 for details), while the Fourier spectra generally include all harmonics $n\omega_i$ ($n = 0, \pm1, \pm2, \ldots$), as well as all combination frequencies $\sum n_i\omega_i$ ($n_i = 0, \pm1, \pm2, \ldots$). Section 3 will be devoted to autoresonant excitation of single-phase SG waves and the diagnostics of this excitation process in terms of the spectral IST problem. Later, we will discuss autoresonant excitation of multiphase SG waves (Section 4) and multiresonant control of the modulational instability (Section 5). Finally, our conclusions will be summarized in Section 6.

2. The spectral problem

The unperturbed ($\epsilon = 0$) SG equation (2) is associated with the matrix scattering problem (we follow the theory in Ref. [4])

$$\frac{dF}{dx} = UF, \tag{3}$$

where

$$U(E,x) = \frac{i}{4}(u_t + u_x)\begin{pmatrix} -1 & 0 \\ 0 & 1 \end{pmatrix} + \frac{1}{16\sqrt{E}}\begin{pmatrix} 0 & -e^{-iu} \\ e^{iu} & 0 \end{pmatrix} - \sqrt{E}\begin{pmatrix} 0 & -1 \\ 1 & 0 \end{pmatrix}. \tag{4}$$

In the periodic case, $u(x) = u(x + L)$, the scattering problem (3) defines a discrete spectrum of complex eigenvalues E_j, when eigenfunctions $F(x, E_j)$ periodic or antiperiodic in $x \in [0, L]$: $F(x + L, E_j) = \pm F(x, E_j)$. On the other hand, a given spectrum E_j defines the solution $u(x)$ uniquely by the inverse scattering problem for (3). In addition, the spectrum yields a multiphase decomposition of the solution, i.e., for a finite (even) number of eigenvalues $\{E_j\}_{j=1}^{j=2N}$ in the problem, the solution assumes the form

$$u(x,t) = u(\Theta_1, \ldots, \Theta_N), \qquad \Theta_i = \kappa_i x - \omega_i t + \Theta_{0i}, \tag{5}$$

where the set of wave vectors κ_i are

$$\kappa_i = 2\pi m_i/L \tag{6}$$

with some integers m_i, while the frequencies ω_i can be calculated via contour integrals defined by the locations of spectral points E_j in the complex spectral plane [15]. We will sort the spectral points in pairs

$$\{E_{2i-1}, E_{2i}\}, \quad i = 1, \ldots, N, \tag{7}$$

with each pair being either complex conjugate ($E_{2i-1} = E_{2i}^*$) or real negative ($E_{2i-1} < E_{2i} < 0$). The case of the complex conjugate pairs comprises the so called "non-soliton" part of the spectrum.

Importantly, the IST spectrum is a dynamic invariant of the unperturbed SG equation and, therefore, the frequencies are independent in time. Thus, the solution with a finite spectrum is periodic in x, but it may be quasiperiodic in t, because the frequencies are generally incommensurate. The frequencies of the multiphase solutions will comprise important characteristics in studying the autoresonance phenomenon in the following, and, therefore, the description of the solutions in terms of the spectrum of the scattering problem (3), (4) is the most adequate technique in analyzing the autoresonance in the SG problems. As an example, we consider the zero solution, $u = 0$, first. Using the substitution

$$F = F_0 e^{ikx}, \quad k = \frac{\pi}{L}n, \; n = 0, \pm1, \pm2, \ldots \tag{8}$$

for periodic (even values on n) and antiperiodic (odd n) eigenfunctions in the scattering problem (3), (4), one obtains the spectrum

$$E(k) = \frac{1}{2}\left(k^2 + \frac{1}{8}\right) \pm \frac{1}{2}\sqrt{\left(k^2 + \frac{1}{8}\right)^2 - \frac{1}{64}}. \tag{9}$$

The spectrum is located on the positive part of the real axis of the complex spectral plane. Each spectral point $E(k)$ is doubly degenerate and represents *closed gaps* (7) ($E_{2i-1} = E_{2i}$) indicating inactive (dormant) degrees of freedom.

A nonzero periodic SG solution is associated with the opening of the closed gaps, as some degenerate points split into pairs of complex conjugate values ($E_{2i-1}^* = E_{2i}$). Here and below we will sort the eigenvalues by associating the wave number k in (9) with the number i of the gap: $i = 1$ for $n = 0$ and, if n is non-zero, $i = 2|n|$ for the positive sign in Eq. (9) and $i = 2|n| + 1$ for the negative sign. Index i enumerates gaps so that for even i we have $E \geq 1/16$ and, for odd i, $0 < E < 1/16$.

Returning to the perturbed SG equation (2), we seek excitation of multiphase solutions of (2) from zero by adding a small driving term ($\epsilon \ll 1$). We wish to open some initially closed gaps in a controllable way, which is the main goal of this study. We will restrict ourselves to the excitation of solutions with the non-soliton spectrum only. We will adopt the usual assumption of the perturbation theory of integrable equations [17,18] associated with the scattering problem (3), (4) that the IST spectrum $E_j(t)$ slowly evolves on time due to perturbations. The technique of computing the spectrum is presented in Appendix A for completeness, while the frequencies are computed by using the approach of Ref. [15]. The details of the algorithm for computations of the associated contour integrals in the spectral plane are presented in Appendix B.

3. Autoresonant excitation of one-phase waves

The simplest solution of the unperturbed SG equation with a one-phase spectrum is a *flat* wave with $u_x = 0$. In this case, Eq. (2) transforms into the pendulum equation with the solution of form

$$u(t) = 2\sin^{-1}[\nu\ \mathrm{sn}(t;\nu)], \quad 0 \leq \nu \leq 1, \tag{10}$$

which is periodic in time with period $4K(\nu)$ and amplitude of oscillations $u_0 = 2\sin^{-1}\nu$. The IST spectrum of this solution is

$$E(k) = \frac{1}{2}\left(k^2 + \frac{1}{8}\cos u_0\right) \pm \frac{1}{2}\sqrt{\left(k^2 + \frac{1}{8}\cos u_0\right)^2 - \frac{1}{64}}, \tag{11}$$

where k is defined in (8). The spectrum is located on the positive real axes and on the circle $|E| = 1/16$.

If $u_0 = 0$, the spectrum transforms into (9). The increase of u_0 leads to opening of the closed gap $E(k = 0) = 1/16$ and the appearance of the nondegenerate complex conjugate pair. A further increase of u_0 leads to formation of a new complex pair if $\cos u_0 < 1 - 8\pi^2/L^2$, but these new spectral points will be doubly degenerate. For even larger u_0, additional spectral points move to the circle $|E| = 1/16$ and all such points are doubly degenerate as well. It is known [15,16] that the single phase wave is modulationally unstable if the spectrum has degenerate points outside the real axis. Thus, the flat wave will be stable only if

$$\cos u_0 \geq 1 - 8\pi^2/L^2. \tag{12}$$

This rule is preserved in a more general case [15,16] of single-phase traveling waves and multiphase waves, i.e. the waves are modulationally unstable if their spectrum contains degenerate points outside the real axes.

Next, we describe our approach to excitation of single-phase waves by using the autoresonance method. We start from zero

Author's personal copy

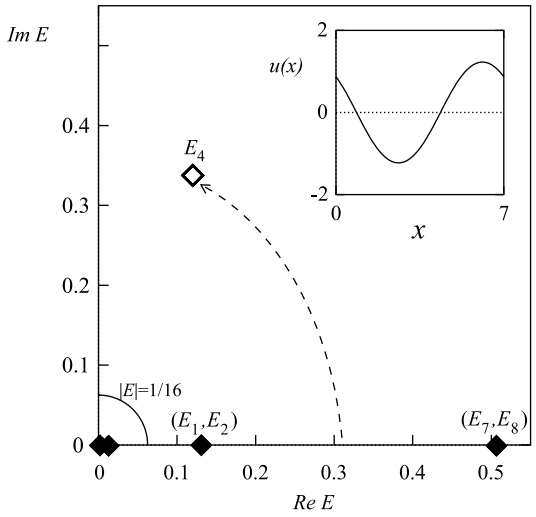

Fig. 1. The spectrum of the excited one-phase traveling wave at $t = 3500$; ◊ – nondegenerate spectral points, ♦ – double degenerate spectral points; $L = 7$, $m = 1$, $\Omega_{01} = 1.344$, $t_0 = 1000$, $\epsilon = 0.003$, $\alpha = 0.00003$. The insert shows the shape of the wave at t_0.

initial conditions and add a perturbation in the form of a small amplitude plane wave

$$f(x,t) = \cos\left(\kappa_m x + \int \Omega_m(t)\mathrm{d}t\right), \qquad \kappa_m = \frac{2\pi}{L}m, \tag{13}$$

where m is an integer. The driving frequency $\Omega_m(t)$ is assumed to be a slowly varying function of time

$$\Omega_m(t) = \Omega_{0m} - \alpha(t - t_0), \tag{14}$$

which passes (at time t_0) the natural frequency of the linearized, unperturbed sine-Gordon equation $u_{tt} - u_{xx} + u = 0$:

$$\Omega_{0m} = \sqrt{1 + \kappa_m^2}. \tag{15}$$

We will assume $\Omega_{0m} > 0$, but κ_m may have an arbitrary sign controlling the opening of different initially closed gaps (9) in the interval $0 < E < 1/16$ if $\kappa_m < 0$ or with $E \geq 1/16$ if $\kappa_m \geq 0$. The number of the affected (opened) gap in the process of excitation is

$$i = \begin{cases} 2m, & m > 0 \\ -2m + 1, & m \leq 0. \end{cases}$$

In particular, if $m = 0$, one can excite a flat wave discussed above. The results of numerical simulations of autoresonant excitation of a single-phase wave with $m = 1$ is shown in Fig. 1. The initially closed gap with $i = 2$ ($E_3 = E_4 = 0.314$) was opened after passage through resonance, as shown by the dashed arrow in Fig. 1. We show the spectral points with even numbers in the upper half-plane, $\mathrm{Im}E_{2i} \geq 0$. The excited traveling waveform at a particular time is shown in the insert in Fig. 1. The wave moves to the left by preserving its form. It is convenient to use the angle $\theta = \arg(E_{2i})$ for characterizing the process of opening of the gap. When this angle increases, the amplitude of the excited wave grows as well. We show θ in our example in Fig. 2. The efficient excitation starts just after the driving frequency crosses the linear resonance at $t = t_0 = 1000$ and continues until the wave is modulationally stable.

The evidence on the autoresonant phase-locking in our system can be obtained by calculating the frequencies $\omega_j(t)$ of the wave. We use the IST spectrum in these calculations below (see the details of the method in Appendices A and B). The evolution of the frequency ω_2 of the excited wave ($m = 1$) associated with the open gap $i = 2$, is shown in Fig. 3 by solid line 1. Prior crossing

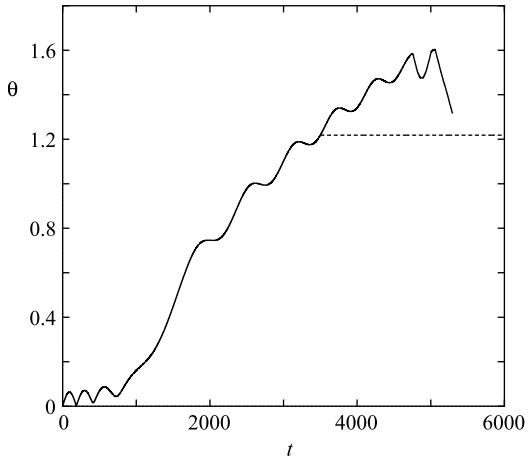

Fig. 2. The opening of the driven gap. The solid line represents the angular width of the opening gap $\theta = \arg(E)$, the dotted line corresponds to the stationary wave solution established after the driving perturbation was switched off at $t = 3500$. The parameters are $L = 7$, $m = 1$, $\Omega_{01} = 1.344$, $t_0 = 1000$, $\epsilon = 0.003$, and $\alpha = 0.00003$.

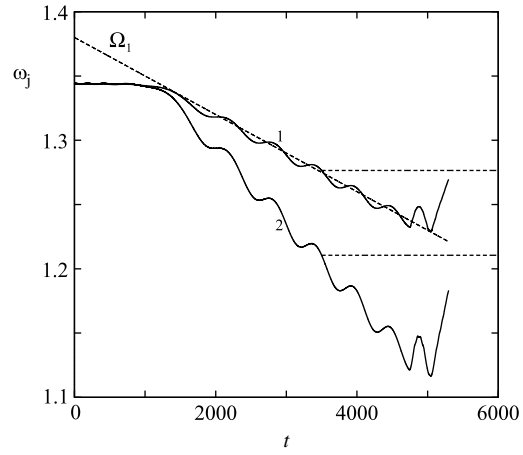

Fig. 3. The evolution of the frequencies ω_j of two adjoint waves. Line 1 is $\omega_2(t)$ of the driven phase-locked wave, line 2 is $\omega_3(t)$, and the dotted lines correspond to the stationary wave established after the driving perturbation is switch off at $t = 3500$; The driving parameters are the same as in Fig. 2.

the resonance ($t < t_0 = 1000$) in the Figure, a small amplitude excited wave has the frequency close to the linear resonance frequency $\omega_2 \approx \Omega_{01} = 1.344$, but beyond the resonance, $\omega_2(t)$ slowly follows the driving frequency $\Omega_1(t)$, i.e. the system is phase-locked. The phase-locking is preserved until the wave is modulationally stable. Line 2 in Fig. 3 shows the evolution of the frequency associated with the closed gap, $i = 3$, which has the same linear resonance frequency, but negative wave number ($m = -1$). This frequency varies in time as the system evolves in autoresonance, but no phase-locking is observed at this frequency and the corresponding gap remains closed. The dotted lines at $t > 3500$ in Figs. 2 and 3 correspond to the stationary traveling wave emerging after the drive is switched off at $t = 3500$. This wave is stable for unlimited time, illustrating the use of autoresonance for efficient excitation of modulationally stable unperturbed solutions of Eq. (2).

Another characteristic of autoresonance is the existence of a threshold on the driving amplitude for nonlinear phase locking transition in passage through the linear resonance at a given driving frequency chirp rate α. We illustrate this effect in simulations in Fig. 4, showing that the transition to autoresonance occurs for $\epsilon > \epsilon_{cr} = 5.1\alpha^{3/4}$. This result is in excellent

Author's personal copy

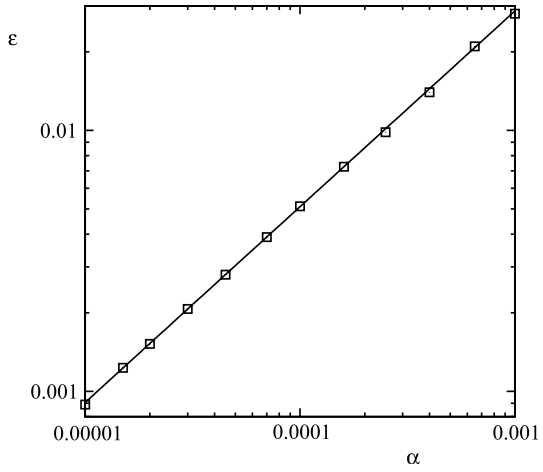

Fig. 4. The threshold for autoresonant phase-locking found numerically (boxes) and the theoretical prediction $\epsilon = 5.1\alpha^{3/4}$ (solid line). The parameters are $L = 7$, $m = 1$, and $t_0 = 1000$.

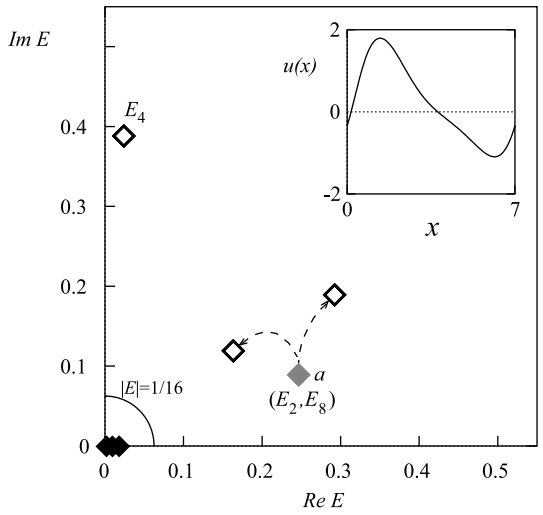

Fig. 5. The IST spectrum of the three-phase wave at $t = 4800$ after the development of the modulational instability. The point a is the doubly degenerate eigenvalue in the initial stage of the modulational instability at $t = 4200$; ◊ describes nondegenerate spectral points and ♦ represents doubly degenerate spectral points. The parameters are $L = 7$, $m = 1$, $\Omega_{10} = 1.344$, $t_0 = 1000$, $\epsilon = 0.003$, and $\alpha = 0.00003$. The insert shows the waveform at time $t = 4800$.

agreement with our theory presented in Appendix C and predicting $\epsilon_{cr} = 3.28(1 + k^2)^{3/4}\alpha^{3/4}$.

The development of the modulational instability in simulations at a later stage of autoresonant evolution is illustrated in Fig. 5. The Figure shows the result of the collision of two points (E_1, E_2) and (E_7, E_8) and formation of a doubly degenerate point a in the upper half-plane. Later this point splits into two nondegenerate points as shown by the arrows in the Figure. Thus, a complex, three-phase wave emerges due to modulational instability, but the phase-locking at this stage is destroyed.

4. Excitation of multiphase waves

In this section, we discuss excitation of multiphase waves by a step-by-step process such that, at the each stage, the drive is a single plane wave of form (13). We have seen in the last Section (see Fig. 3) that in autoresonance, all frequencies ω_j, including those different from the driving frequency, experience a slow drift. This drift introduces a need of evaluation of the resonant frequencies when applying new driving waves in

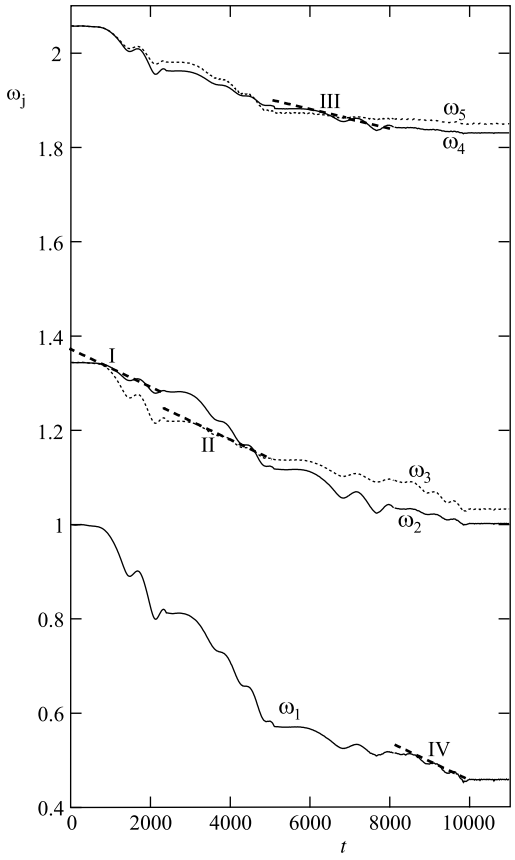

Fig. 6. The evolution of the frequencies ω_j in four successive stages of excitation of a four-phase wave. In stage I, $m = 1$, $\epsilon = 0.003$, $\alpha = 0.00004$, $\Omega_{0m} = 1.34$, and $t_0 = 800$. In stage II, $m = -1$, $\epsilon = 0.003$, $\alpha = 0.00004$, $\Omega_{0m} = 1.22$, and $t_0 = 3000$. In stage III, $m = 2$, $\epsilon = 0.003$, $\alpha = 0.00002$, $\Omega_{0m} = 1.88$, and $t_0 = 6000$. In stage IV, $m = 0$, $\epsilon = 0.002$, $\alpha = 0.00004$, $\Omega_{0m} = 0.51$, and $t_0 = 8700$. The thick dashed lines show the evolution of the driving frequencies $\Omega_m(t)$.

subsequent excitation stages. The new resonant frequencies can differ significantly from the linear resonance frequencies (15) in the problem. The advantage of our approach is that one can follow the frequencies of all phases in the solution, including inactive degrees of freedom and, thus, define all resonant frequencies Ω_{0m} for subsequent stages in the process of evolution. At each time the frequencies of inactive phases describe small perturbations of these degrees of freedom on the background of a high amplitude wave excited in the previous excitation stage. We illustrate these ideas showing a numerical example of a four-step autoresonant excitation process in Fig. 6. We drive our system successively by small amplitude, chirped frequency waves with wave vectors $\kappa_m = \frac{2\pi}{L}m$, $m = 1, -1, 2, 0$. The initial resonant frequencies at each excitation stage are evaluated via the IST at the end of the previous step. In addition, by following the spectrum in the complex plane, we avoid the modulational instability by introducing new drives prior a degenerate point appears outside the real axis of the spectral plane. The successive opening of the closed gaps during this excitation process of a multiphase wave is illustrated in Fig. 7.

An interesting result is been obtained at the intermediate stage ($t \approx 4600$). At this time the two-phase solution was excited having degenerate frequencies $\omega_2 \approx \omega_3$. At the same time the spectrum assumes a special symmetry $E_6 = E_4/16$. A similar wave was excited in Ref. [9] by a different type of driving and comprised a plasma oscillation, i.e. a nonlinear standing waveform illustrated in Fig. 8 at the three nearly equal times. Thus, we have demonstrated that plasma oscillations can be also excited by in step-by-step process.

Author's personal copy

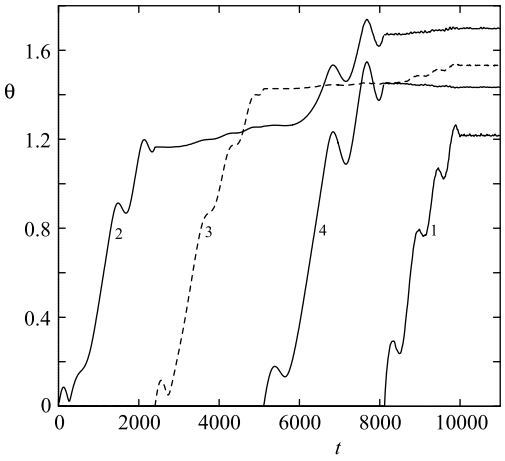

Fig. 7. The opening of the driven gaps in the process of successive excitation of four phases. The numbers of the curves correspond to the numbers of the frequencies in Fig. 6.

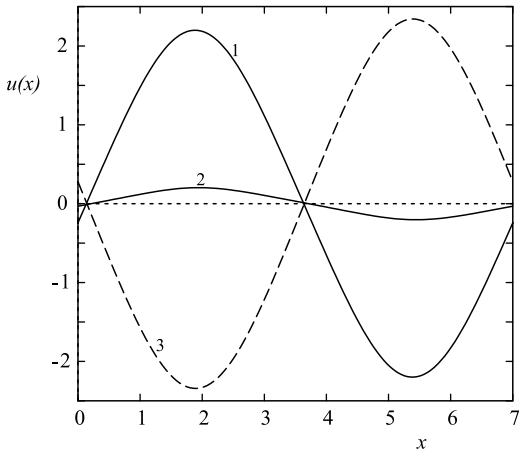

Fig. 8. The waveform of the plasma oscillations in the intermediate stage of the process of excitation of a two-phase solution. Line 1 corresponds to $t = 4611.3$, line 2 is at $t = 4613.0$, and line 3 at $t = 4614.7$.

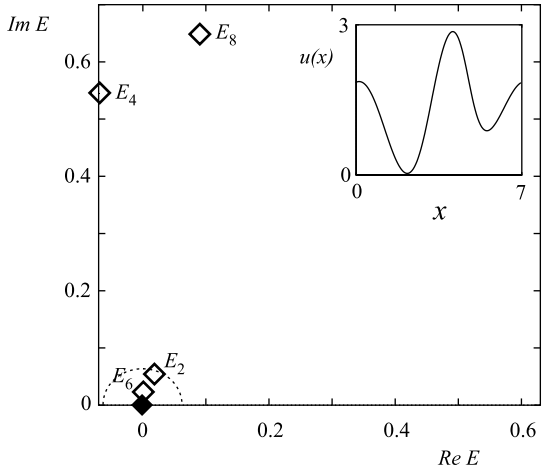

Fig. 9. The spectrum of the four-phase wave at $t = 10\,000$. ◊ represents nondegenerate spectral points and ♦ are doubly degenerate spectral points. The insert shows the actual waveform at the same time.

At the last (fourth) stage of excitation shown in Fig. 6 we switched off the drive at $t = 10\,000$ and observed a stable four-phase solution having the spectrum and the instantaneous form shown in Fig. 9.

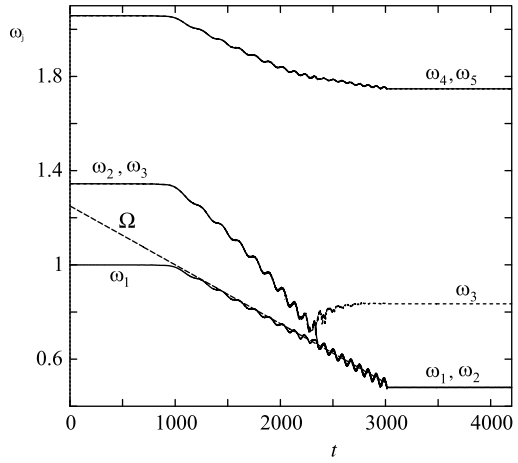

Fig. 10. The evolution of the frequencies ω_j in the multiphase excitation of the periodic SG breather solution. The parameters are $\epsilon = 0.012, \alpha = 0.00025, \Omega_0 = 1$, and $t_0 = 1000$.

5. Multiphase driving and control of the modulational instability

The single-phase multi-step driving process described above allows one to excite only waves having a linear limit, plasma oscillations for example. But the SG equation has more complex solutions, having no linear limit. One of the most famous such solutions is a breather. As shown in Ref. [9], one can excite a breather by combined chirped frequency drives when passing through the modulational instability of a large amplitude plane wave. The spectral analysis of this process of excitation of breathers and control of the modulational instability by autoresonant drives are the main goals of this section.

We will use the same form of the driving perturbation as in Ref. [9]:

$$f(x,t) = [1 + r\cos(\kappa x)]\cos\left(\int \Omega(t)\mathrm{d}t\right). \tag{16}$$

This is a combination of an oscillation and a standing wave, i.e. a three-phase drive in terms of Eq. (13) with a chirped common frequency

$$\Omega(t) = \Omega_0 - \alpha(t - t_0) \tag{17}$$

and wave numbers $\kappa_0 = 0$, $\kappa_1 = \kappa$ and $\kappa_{-1} = -\kappa$. We start from zero set $\Omega_0 = 1$ and $r = 0$ in Eq. (16) at $t < t_0$ for avoiding resonances involving spatial harmonics during the initial excitation process, but switch to $r = 1$ at $t \geq t_0$. The process of the excitation of the SG wave in this case in simulations is illustrated in Figs. 10 and 11. At $t \approx t_0$ the driving perturbation crosses the resonance with the SG oscillation having $\Omega \approx 1$ and leads to the opening of gap $i = 1$ corresponding to $m = 0$ mode (see Fig. 11, line 1). As the driving frequency decreases beyond the linear resonance, the driven SG oscillation remains phase-locked, i.e. the system stays in autoresonance. At the same time, the frequencies ω_2 and ω_3 of the inactive degrees of freedom corresponding to modes $m = \pm 1$, decrease in time, until crossing the driving frequency. Immediately after this crossing one observes a bifurcation, accompanied by the opening of the gap associated with mode $m = 1$, continuing phase locking of this mode, and growth of its amplitude (see Fig. 11). The mode $m = -1$ is not phase-locked and the corresponding gap $i = 3$ is not opened. As the result, a large amplitude quasi-single-phase wave ($\omega_1 \approx \omega_2$) emerges and remains stable after the drive is switched off at $t = 3000$.

Author's personal copy

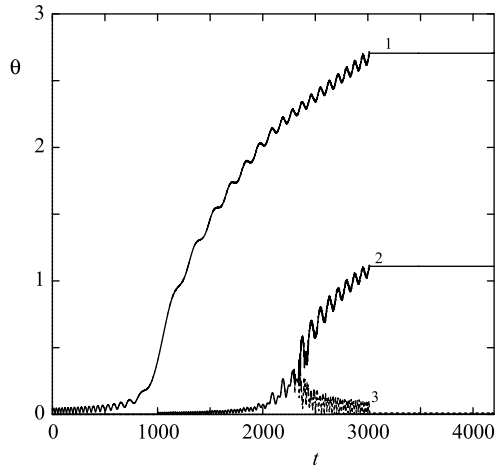

Fig. 11. The opening of the driven gaps in the process of multiphase excitation of the breather solution. The numbers of the curves correspond to numbers of the frequencies in Fig. 10.

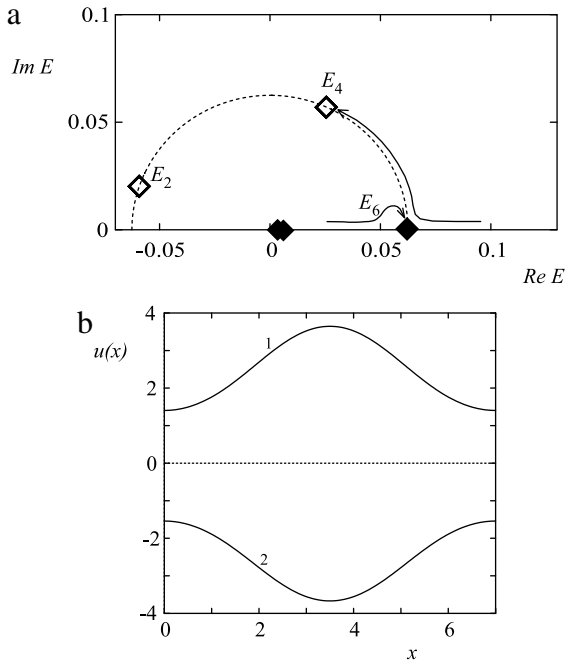

Fig. 12. The autoresonant SG breather solution.(a) The spectrum of the breather solution at $t = 4200$, ◊ describes the nondegenerate spectral points and ♦ corresponds to the doubly degenerate spectral points. (b) The actual waveform of the breather (line 1 at $t = 3973.2$ and line 2 at $t = 3978.4$).

The IST spectrum of this excitation process is illustrated in Fig. 12(a). The perturbations of modes $m = \pm 1$ lead to the removal of the degeneracy of gaps (E_3, E_4) and (E_5, E_6) adding small, $O(\epsilon)$, imaginary parts in the spectrum. The evolution of the spectral points E_4 and E_6 in the upper half-plane in Fig. 12(a) is shown by the arrows. The points move closer to each other prior the bifurcation, while after the bifurcation, E_4 moves upward along the circle $|E| = 1/16$ and E_6 approaches the real axis. As the result, after switching off the driving, one obtains a standing breather solution with the characteristic spectrum consisting of two open gaps with the spectral points located on the circle $|E| = 1/16$. All other gaps remain closed. Formally, the breather is a two phase solution with degenerate frequencies $\omega_1 = \omega_2$. Fig. 12(b) shows the form of this stable standing wave. The bifurcation point discussed above is associated with the modulational instability of the plain wave and the removal of the degeneracy by additional driving components ($r \neq 0$ in Eq. (16)) yields a possibility of controlling this instability and formation of a breather. Without this additional components the phase locking in the driven system is destroyed as one passes the modulationally unstable point, resulting in formation of a complex three-phase solution as seen in Section 3. Finally, we did not observe any chaotic behavior in our chirped driving frequency simulations similar to those seen with constant frequency driving [6], because, shortly after passing the threshold for modulational instability of a plane wave, a modulationally stable, driven breather solution was formed.

6. Conclusions

In conclusion:

(a) We have discussed the problem of autoresonant excitation and control of multiphase solutions of the periodic sine-Gordon problem. The autoresonance is a unique property of many nonlinear systems to stay in resonance with oscillating driving perturbations, despite variation of system parameters. In the autoresonance state of the system is controlled by variation of external parameters.

(b) The periodic sine-Gordon problem allows general multiphase solutions, with a finite number of phases, each characterized by its wave vector and frequency. The formation of such solutions requires a realization of complicated initial conditions, which makes the formation of multiphase waves with prescribed properties in physical applications difficult. In this context, the autoresonance comprises a physically realizable path to multiphase solutions. Indeed, we have shown that the autoresonant state in the SG case is reached by starting from zero and applying simple, chirped frequency wave-like perturbations passing through resonances with inactive (dormant) phases in the problem. By using different drives successively, one can use the autoresonance of each newly formed phase for controlling the emerging multiphase solution by varying the driving frequency.

(c) We have analyzed this excitation process by using the IST method. The approach allows to verify the phase-locking in the system at each excitation stage, as well as to predict the driving parameters (driving frequency) in a subsequent excitation stage. We have illustrated our approach in simulations, showing the formation of a single-phase autoresonant traveling wave in the first excitation stage, followed by emergence of two-, three-, and four-phase SG waves as new drives are applied at each stage.

(e) We have found that similar to many other applications, the successful autoresonance in the system requires the driving amplitude to exceed a threshold, which scaled as 3/4 power of the driving frequency chirp rate. We have found this threshold analytically in the fist excitation stage (formation of a traveling single-phase wave) and the analytic result was in an excellent agreement with simulations.

(f) In the aforementioned step-by-step process of autoresonant formation of multiphase waves one must avoid modulational instabilities when the IST spectral points collide in the complex spectral plane. Typically, such collisions lead to destruction of autoresonance and loss of control of the driven wave. Nevertheless, the simultaneous application of several driving perturbations in some cases allows one to control the modulational instability. For example, driving the system by a combination of a chirped frequency oscillation and a standing wave yields formation of a flat wave, which later, after passing through the modulational instability, transforms into the autoresonant SG breather.

Acknowledgments

This work was supported by the US–Israel Binational Science Foundation, grant no. 2004033.

Author's personal copy

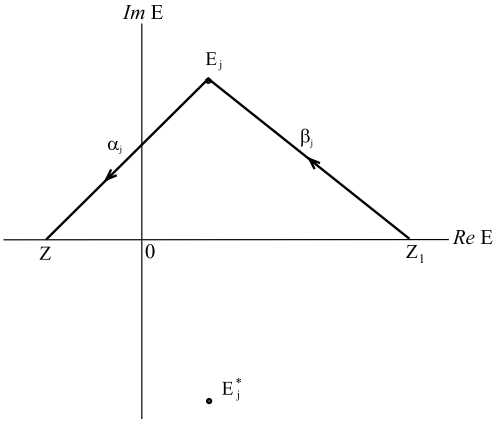

Fig. 13. Contours of integration in spectral plane.

Appendix A. The IST spectrum

Let $\{x_n\}_{n=0}^{M}$ be the grid in the interval $[0, L]$ with step $h = L/M$, i.e. $x_n = hn$. Then, the transfer matrix at given t can be computed by solving the ODE (3) numerically, subject to initial condition at $x = 0$

$$F^0 = \begin{pmatrix} 1 & 0 \\ 0 & 1 \end{pmatrix}. \tag{A.1}$$

We use $O(h^2)$ algorithm in this calculation, i.e.

$$F^{n+1} = F^n + \frac{h}{2}[U(x_n)F^n + U(x_{n+1})(1 + hU(x_n))F^n] \tag{A.2}$$

where $n = 0, 1, \ldots, M-1$ and $U(x_n)$ is the value of the matrix (4) on the grid point x_n. The transfer matrix F^M depends on E as a parameter. The Floquet discriminant is the trace of the transfer matrix

$$\Delta(E) = \mathrm{tr}(F^M). \tag{A.3}$$

The discrete spectrum $\{E_j\}$ corresponds to the solutions of the implicit equation $\Delta(E) = \pm 2$.

Appendix B. Frequencies of multiphase SG waves

Here we calculate the frequencies ω_i associated with different phases in the SG solutions [15]. The calculation requires computation of the following singular integrals in the complex plane of the spectral parameter E

$$A_{kj} = 4\ Re\left(\int_{\alpha_j} \frac{E^{N-k}dE}{R(E)}\right), \quad k, j = 1, \ldots, N, \tag{B.1}$$

$$B_{kj} = 2\ Re\left(\int_{\alpha_j} \frac{E^{N-k}\mathrm{d}E}{R(E)}\right) + 2\mathrm{i}\ \mathrm{Im}\left(\int_{\beta_j} \frac{E^{N-k}\mathrm{d}E}{R(E)}\right), \tag{B.2}$$

where $R^2(E) = E\prod_{l=1}^{2N}(E - E_l)$ and contours of integration are shown in Fig. 13. One notes that the real parameters $Z < 0$ and $Z_1 > Re(E_j)$ may be arbitrary, but the contours cannot cross the spectral points. The integrals define $N \times N$ matrixes A and B. The next step is the solution of the matrix equation

$$A^{\mathrm{T}}C = I, \tag{B.3}$$

where I is the unit matrix. Introducing the matrix $F = C(A - 2B)$, one computes the N frequencies from [15]

$$\omega_j = \sum_{k=1}^{N} 4\pi\mathrm{i}(F^{-1})_{kj}\left(C_{k1} + \frac{(-1)^{N-1}C_{kN}}{16\sqrt{\prod_{l=1}^{2N} E_l}}\right). \tag{B.4}$$

The key problem in the algorithm described above is the computation of the singular integrals. We illustrate this computation of the first integral (B.1). We rewrite the integral by extracting the non-singular part

$$A_{kj} = 4\ Re\left(\int_{E_j}^{Z} \Phi(E, k)\frac{\mathrm{d}E}{\sqrt{E - E_j}}\right). \tag{B.5}$$

Then, by substitution

$$E = E_j + (Z - E_j)\theta^2, \quad \theta \in [0, 1], \tag{B.6}$$

the integral takes a non-singular form

$$A_{kj} = 8\ Re\left(\sqrt{Z - E_j}\int_0^1 \Phi(\theta, k)\mathrm{d}\theta\right). \tag{B.7}$$

Appendix C. The threshold condition

In this Appendix we use the Whitham's averaged variational principle [20,7] in calculating the threshold for autoresonant transition of single phase SG waves. We proceed from the Lagrangian for a single phase wave (of wave vector κ) in the driven weakly nonlinear SG problem

$$L = \frac{1}{2}(u_t^2 - \omega_0^2 u^2) + \frac{1}{24}u^4 + \epsilon u\cos\theta_d, \tag{C.1}$$

where $\omega_0^2 = k^2 + 1$, the driving phase is $\theta_d = \kappa x - \int \Omega(t)\mathrm{d}t$, and $\Omega(t) = \omega_0 - \alpha t$ is the chirped driving frequency. Here, we substitute the *ansatz* $u = a\cos\theta$ and average over θ between 0 and 2π yielding the averaged Lagrangian

$$\Lambda(a, \theta, \theta_t) = \frac{1}{4}(\omega^2 - \omega_0^2)a^2 + \frac{1}{64}a^4 - \frac{1}{2}\epsilon a\cos\Phi. \tag{C.2}$$

Here a and θ are the dependent variables, $\omega = -\theta_t$ is the frequency of the driven wave, $\Phi = \theta - \theta_d$ is the mismatch between the driven and driving waves, and we neglect the contribution from the nonresonant driving component $\frac{1}{2}\epsilon a\cos(\theta + \theta_d)$. The variational equations obtained from (C.2) by taking variations with respect to the wave amplitude a and phase θ are

$$(\omega^2 - \omega_0^2)a + \frac{1}{8}a^3 - \epsilon\cos\Phi, \tag{C.3}$$

$$(\omega a^2)_t = \epsilon a\sin\Phi. \tag{C.4}$$

Next, we approximate $\omega \approx \omega_0$, $\omega^2 - \omega_0^2 \approx 2\omega_0(\omega - \omega_0)$ allowing to rewrite Eqs. (C.3) and (C.4) as

$$\Phi_t = \alpha t - \frac{1}{16\omega_0}a^2 + \frac{\epsilon}{2a\omega_0}\cos\Phi, \tag{C.5}$$

$$a_t = \frac{\epsilon}{2a\omega_0}\sin\Phi, \tag{C.6}$$

which, after rescaling, $\tau = \alpha^{1/2}t$, $a' = \frac{1}{4}\alpha^{-1/4}\omega_0^{-1/2}a$, and introducing $\mu = \frac{\epsilon}{8}(\omega_0^2\alpha)^{3/4}$ becomes

$$\Phi_\tau = \tau - a'^2 + \frac{\mu}{a'}\cos\Phi, \tag{C.7}$$

$$a'_t = \mu\sin\Phi. \tag{C.8}$$

Finally, by introducing complex dependent variable $\psi = a'\exp(\mathrm{i}\Phi)$, we rewrite this system as a single nonlinear Schrodinger-type equation

$$\mathrm{i}\psi_\tau + (|\psi|^2 - \tau)\psi = \mu. \tag{C.9}$$

Author's personal copy

The passage through resonance in this equation corresponds to starting from $\psi = 0$ at $\tau = -\infty$ and seeking an asymptotic solution for ψ at $\tau = +\infty$. It is the single parameter μ in this system that controls the autoresonant phase locking transition, which occurs for $\mu > \mu_{cr} = 0.41$ [19]. By returning to our original parameters, we arrive at the threshold condition on the driving amplitude

$$\epsilon > \epsilon_{cr} = 3.28\omega_0^{3/2}\alpha^{3/4}. \tag{C.10}$$

References

[1] A. Scott, Nonlinear Science: Emergence and Dynamics of Coherent Structures, Oxford University Press, Oxford, 1999.
[2] G.L. Lamb Jr., Rev. Modern Phys. 43 (1971) 99.
[3] G. Costabile, R.D. Parmentier, B. Savo, D.W. McLaughlin, Exact solutions of the sine-Gordon equation describing oscillations in a long (but finite) Josephson junction, Appl. Phys. Lett. 32 (1978) 587–589.
[4] S.P. Novikov, S.V. Manakov, L.P. Pitaevsky, V.E. Zakharov, Theory of Solitons, Consultants Bureau, New York, 1984.
[5] M.G. Forest, D.W. McLaughlin, Spectral theory for the periodic sine-Gordon equation: A concrete viewpoint, J. Math. Phys. 23 (1982) 1248–1277.
[6] A.R. Bishop, M.G. Forest, D.W. McLaughlin, E.A. Overman, Physica D 23 (1986) 293.
[7] L. Friedland, Autoresonant excitation and evolution of nonlinear waves: The variational approach, Phys. Rev. E 55 (1997) 1929–1939.
[8] L. Friedland, Autoresonance of coupled nonlinear waves, Phys. Rev. E 57 (1998) 3494–3501.
[9] L. Friedland, A.G. Shagalov, Emergence and control of breather and plasma oscillations by synchronizing perturbations, Phys. Rev. E. 73 (2006) 066612.
[10] J. Fajans, L. Friedland, Autoresonant (nonstationary) excitation of pendulums, Plutinos, plasmas, and other nonlinear oscillators, Amer. J. Phys. 69 (2001) 1096–1102.
[11] A.I. Nicolin, M.H. Jensen, J.W. Thomsen, R. Carretero-Gonzalez, Resonant energy transfer in Bose–Einstein condensates, Physica D 237 (2008) 2476–2481.
[12] G. Manfredi, P.A. Hervieux, Autoresonant control of the many-electron dynamics in nonparabolic quantum wells, Appl. Phys. Lett. 91 (2007) 061108.
[13] H. Maeda, J. Nunkaew, T.F. Gallager, Classical phase-locking in adiabatic rapid passage, Phys. Rev. A 75 (2007) 053417.
[14] L. Friedland, A.G. Shagalov, Excitation of multiphase waves of the nonlinear Schrodinger equation by capture into resonances, Phys. Rev. E 71 (2005) 036206.
[15] R. Flesch, M.G. Forest, A. Sinha, Numerical inverse spectral transform for the periodic sine-Gordon equation: Theta function solutions and their linearized stability, Physica D 48 (1991) 169–231.
[16] N. Ercolani, M.G. Forest, D.W. McLaughlin, Geometry of the modulational instability, Physica D 43 (1990) 349–384.
[17] I.M. Krichever, Hessians of integrals of the Korteweg–de Vries equation and perturbations of finite gap solutions, Sov. Math. Dokl. 270 (1983) 1312–1317.
[18] V.I. Karpman, E.M. Maslov, V.V. Solov'ev, Dynamics of bions in long Josephson junction, Sov. Phys. JETP 57 (1983) 167–173.
[19] G. Marcus, L. Friedland, A. Zigler, From quantum ladder climbing to classical autoresonance, Phys. Rev. A 69 (2004) 013407.
[20] G.B. Whitham, Linear and Nonlinear Waves, Willey, New York, 1974.